

# A Review of Advances in Groundwater Evapotranspiration Research

Xianglong Hou <sup>1</sup>, Hui Yang <sup>2</sup> , Jiansheng Cao <sup>2,\*</sup>, Wenzhao Feng <sup>2,3</sup> and Yuan Zhang <sup>1,\*</sup>

<sup>1</sup> Institute of Geographical Sciences, Hebei Academy of Sciences, Hebei Technology Innovation Center for Geographic Information Application, Shijiazhuang 050011, China

<sup>2</sup> Key Laboratory of Agricultural Water Resources, Hebei Key Laboratory of Agricultural Water-Saving, Center for Agricultural Resources Research, Institute of Genetics and Developmental Biology, Chinese Academy of Sciences, Shijiazhuang 050001, China

<sup>3</sup> School of Land Science and Space Planning, Hebei GEO University, Shijiazhuang 050021, China

\* Correspondence: caojis@sjziam.ac.cn (J.C.); 83zhangyuan@sohu.com (Y.Z.)

**Abstract:** Groundwater evapotranspiration ( $ET_g$ ) is an important component of the hydrological cycle in water-scarce regions and is important for local ecosystems and agricultural irrigation management. However, accurate estimation of  $ET_g$  is not easy due to uncertainties in climatic conditions, vegetation parameters, and the hydrological parameters of the unsaturated zone and aquifers. The current methods for calculating  $ET_g$  mainly include the WTF method and the numerical groundwater model. The WTF method often requires data supplementation from the numerical unsaturated model to reduce uncertainty; in addition, it relies on point-monitoring data and cannot solve the spatial heterogeneity of  $ET_g$ . The  $ET_g$  calculation module of the numerical groundwater model is set up too simply and ignores the influence from the unsaturated zone and surface cover. Subsequent research breakthroughs should focus on the improvement of WTF calculation theory and the setting up of an aquifer water-table fluctuation monitoring network. The numerical groundwater model should couple the surface remote sensing data with the unsaturated zone model to improve the accuracy of  $ET_g$  calculation.

**Keywords:** groundwater evapotranspiration; water-table fluctuation method; unsaturated zone; aquifer; MODFLOW; HYDRUS



**Citation:** Hou, X.; Yang, H.; Cao, J.; Feng, W.; Zhang, Y. A Review of Advances in Groundwater Evapotranspiration Research. *Water* **2023**, *15*, 969. <https://doi.org/10.3390/w15050969>

Academic Editor: Adriana Bruggeman

Received: 13 January 2023

Revised: 26 February 2023

Accepted: 28 February 2023

Published: 2 March 2023



**Copyright:** © 2023 by the authors. Licensee MDPI, Basel, Switzerland. This article is an open access article distributed under the terms and conditions of the Creative Commons Attribution (CC BY) license (<https://creativecommons.org/licenses/by/4.0/>).

## 1. Introduction

Water scarcity is already the biggest challenge for global agricultural development [1], with one third of the population in developing countries living in water-scarce areas and fifty-four percent of agricultural land also being located in water-scarce areas [2,3]. In water-scarce areas, groundwater evapotranspiration is an important part of the hydrological cycle; it is one of the main sources of regional evapotranspiration and the main consumer of groundwater in areas with a shallow water table [4,5]. Arid and semiarid regions occupy approximately 30% of the land surface of the Earth [6], including the majority of northern and southern Africa; the Middle East; western USA and southern South America; most of Australia; large parts of central Asia; and parts of Europe [7]. Vegetation provides natural protection against desertification and dust storms in these regions. Some vegetation, known as phreatophyte, is groundwater dependent [8]. Phreatophyte transpiration consumes groundwater and causes diurnal fluctuations of groundwater levels [9]. On the other hand, surface water is scarce, and groundwater is often the only reliable water resource for socio-economic development in arid regions [10]. Irrigation water for crops is usually provided by the abstraction of groundwater. The over-exploitation of groundwater resources has caused decreasing groundwater levels and resulted in desertification in many parts of arid regions [11]. The sustainable management of groundwater resources must consider water use both from human activities and by nature. The starting point to develop a sustainable groundwater use plan is the assessment of groundwater balance. In

arid environments, an important component of the groundwater balance is groundwater evapotranspiration ( $ET_g$ ) [12]. Accurate estimation of groundwater evapotranspiration is essential for understanding hydrological cycle processes and sustainable groundwater resource use and management [13–15], and it is useful for natural ecosystem conservation and restoration [16]. The quantification of groundwater evapotranspiration is particularly important in areas dependent on groundwater ecosystems [17–20] and is important for water management of crops and the investigation of soil salinization processes [21–23].

Groundwater evapotranspiration ( $ET_g$ ) can result in significant loss of groundwater storage.  $ET_g$  is generated when water moves from the unsaturated zone to replenish soil storage depleted by surface evapotranspiration and root water uptake. The shallow water table allows groundwater to be used to directly supply crop growth [24–29], so an accurate estimation of  $ET_g$  for farmland can help to improve irrigation management. Any efforts toward improving  $ET_g$  estimation methods are worthwhile for agricultural water management and land and water environmental protection [15].

However, accurate estimation of groundwater evapotranspiration remains a challenge because it is often influenced by uncertainties associated with climatic variables, vegetation parameters, geological variables, and hydrologic parameters [30,31].

Numerous studies have been conducted on evapotranspiration estimation models worldwide, and these studies have mainly included empirical statistical models, energy balance models, remote sensing models based on Penman's formula, complementary correlation models, and hydrological models. The evapotranspiration model (later called the Food and Agricultural Organization Penman–Monteith (FAO56-PM) model) proposed by Allen [32] is the most suitable model for estimating international evapotranspiration at present, and this model has been widely used worldwide. Evapotranspiration (ET) includes surface evaporation ( $E_s$ ), evaporation of water from below the ground surface ( $E_{ss}$ ), and transpiration of water by plants ( $T_{ss}$ ). The latter two were together defined as subsurface evapotranspiration ( $ET_{ss}$ ) [33], which includes groundwater evapotranspiration ( $ET_g$ ) and unsaturated water evapotranspiration ( $ET_u$ ) [34].

There are many computational methods applied to different scales to calculate evapotranspiration, including the method based on evapotranspiration lysimeter weighing [35–38], the method based on field water balance equations [39–42], micrometeorological methods [16], vorticity covariance methods [43–46], the Bowen ratio method [47], and regional-scale ET calculation models (for example, the TSEB model [48], the SEBAL model [49], the S-SEBI model [50], the SEBS model [51], and the LandSAF model [52]), as well as mapping of evapotranspiration using the internal scale method (METRIC) [53], the STSEB model [54], the GLEAM model [55], the MODIS-ET model [56], and the ETwatch product [57]. However, these methods are usually used more for the measurement and calculation of earth surface evapotranspiration and are not able to directly measure the value of groundwater evapotranspiration, mainly because the hydraulic connection between the earth surface and the aquifer is blocked by the unsaturated zone, and the uncertainty of the unsaturated zone increases the difficulty of calculating groundwater evapotranspiration. Therefore, the calculation of groundwater evapotranspiration often needs to consider the variation of moisture content in the unsaturated zone. In addition to this, the accurate estimation of  $ET_g$  needs to consider the variation of local atmospheric conditions [58] and groundwater table variation [59], and is also influenced by the spatial heterogeneity of land use [60]. Moreover, many factors such as lateral inflow at the recharge boundary, vertical recharge at the surface, and complex geological structure and soil composition in the unsaturated zone can affect  $ET_g$  [61–64]. In addition, intensive anthropogenic measures, such as water diversions and irrigation in water-scarce areas, also have a significant impact on groundwater evapotranspiration. External water transfers directly change the water storage capacity of inland lakes, and overall raise the groundwater table in the wetlands around the lakes and diversion channels. This change in groundwater is continuous, unlike the transfer of water for irrigation in agricultural areas. The shallower water table makes the water storage capacity and regulation capacity of the unsaturated zone weaker, the capillary zone is closer

to the surface, and thus groundwater evapotranspiration becomes stronger; in addition, the shallower water table allows more channels for groundwater to rise into the air, and the root systems of some deep-rooted plants can act directly on the unsaturated zone and even the aquifer. The branches and roots of plants establish the hydraulic connection between air and aquifer, and driven by the transpiration of plants, a large amount of groundwater enters the air directly without passing through the unsaturated zone. The shallower unsaturated zone channels and the newly added plant channels change the proportion of groundwater evapotranspiration ( $ET_g$ ) in total evapotranspiration ( $ET_a$ ). This combination of multiple factors makes  $ET_g$  difficult to calculate.

## 2. Methodology

### 2.1. Advances in Research on Groundwater Evapotranspiration

Historical studies of groundwater evapotranspiration by researchers date back to the 1920s. The early researchers found that groundwater is constantly supplied with evapotranspiration through “capillary rise,” which is evident in groundwater when the water table is less than 3 m. Remson and Fox [65] proposed a method for estimating groundwater discharge by evapotranspiration from the water capillary rise of the water table. “Potential capillary water loss” is defined as a measure of the ability of the soil capillary gap to raise water from the groundwater to the earth surface, and they consider the depth of the water table as the most important factor affecting the magnitude of groundwater evapotranspiration. Gardner’s [66] analysis showed that the evapotranspiration rate depends on the depth of the water table and the capillary flux. Subsequently, Gardner [66] and Willis [67] proposed the calculation of  $ET_g$  as a function of water table depth, and although their assumption of the constant moisture content in the unsaturated zone is inaccurate today, this idea has had a profound impact on subsequent studies of groundwater evapotranspiration. Schoeller [68] introduced the concept of ultimate evapotranspiration depth, and he theorized that groundwater evapotranspiration occurs only when the groundwater table depth is smaller than the ultimate evapotranspiration depth. The magnitude of the groundwater evapotranspiration value is determined by the groundwater table depth together with the potential evapotranspiration value, and this method is widely used because of its simple form. In the classic groundwater numerical model MODFLOW, the groundwater package EVT still follows this idea in the calculation of evapotranspiration. Doorenbos and Pruitt [69] proposed a method to calculate  $ET_g$  by quantifying the variation of soil water content in the root zone. They were the first to elaborate on the relationship between  $ET_g$  and soil moisture in the root zone of crops. This method has been used in soil water balance models for calculating the magnitude of  $ET_g$ . The calculation of soil water balance is a specific application of the water balance equation theory, which is also a common method for groundwater evapotranspiration calculations and is applicable to different scales [4,70–72].

Wang et al. [15] used the water balance equation to calculate the soil water content in the root zone under irrigation and rainfall conditions, and then proposed a new equation that integrates multiple influencing factors to estimate  $ET_g$  during the growing season based on the methods proposed by Doorenbos and Pruitt [69] and the Averianov equation [68]. Groundwater evapotranspiration was calculated using the following equation.

$$ET_g = K_c \times ET_0 \times \left(1 - \frac{H}{H_{\max}}\right)^n \times \frac{\theta_{fc} - \theta}{\theta_{fc} - \theta_r} \quad (1)$$

where  $K_c$  is crop coefficient,  $ET_0$  is reference crop evapotranspiration in  $\text{mm} \cdot \text{day}^{-1}$ ,  $H$  is the actual water table depth in m,  $H_{\max}$  is the potential maximum depth in m, beyond which no  $ET_g$  occurs;  $n$  is the soil characteristics parameter,  $\theta$  is the actual averaged soil water content in the root zone in  $\text{cm}^3 \cdot \text{cm}^{-3}$  (usually about 60 cm below the soil surface),  $\theta_{fc}$  is the field capacity of the soil in the root zone in  $\text{cm}^3 \cdot \text{cm}^{-3}$ ,  $\theta_r$  is the soil water content close to

permanent wilting point in  $\text{cm}^3 \cdot \text{cm}^{-3}$  (in this paper, a constant value 0.05 is used [73]). The method was tested and validated against the data from the lysimeter experiments.

Wang et al. [74] then used the following water balance equation to calculate  $ET_g$  based on  $ET_a$  obtained in a subsequent study.

$$ET_g = (P + I) + \Delta SWC - ET_a - P_c \quad (2)$$

where  $P$  and  $I$  are precipitation and irrigation in mm, respectively,  $\Delta SWC$  is the variation in soil water storage up to 90 cm depth where most of the maize root system is concentrated [75], and  $P_c$  is the deep percolation to shallow groundwater. Since the daily  $\Delta SWC$  was sometimes too small to accurately determine using Hydra probe measurements, the two-day average was used to calculate the water balance. In any event, it was assumed that either  $P_c$  or  $ET_g$  was zero. Lai et al. [76] considered quantifying the contribution of shallow groundwater to evapotranspiration ( $ET_g$ ) as an important topic that has been extensively studied [77,78]. They used lysimeters to calculate groundwater evapotranspiration values for wheat fields in the lower Yellow River basin at different groundwater level conditions. He concluded that reasonable groundwater level control can help increase yields while reducing the risk of soil salinization and is important for sustainable management of the lower Yellow River basin.

## 2.2. Using the WTF Method to Calculate the $ET_g$

Among the methods for calculating groundwater evapotranspiration considering the influence of crops or plant roots, the groundwater table fluctuation (WTF) method is one of the most commonly used methods. In recent decades, there has been an increasing emphasis on using the WTF method to quantify  $ET_g$ . Calculating  $ET_g$  based on the WTF method is a relatively straightforward, simple and inexpensive method [9,79,80]. Users can measure water loss due to evapotranspiration directly from groundwater table changes and therefore does not require additional measurements at the soil surface [73,81–83]. The use of the groundwater table fluctuation method assumes that groundwater table changes in a shallow aquifer are caused by evapotranspiration only [84], and this method has been widely used to estimate  $ET_g$  in riparian zones and wetlands [13,58,85–87].

The method of groundwater table fluctuation exploits the law of daily variation of the water table in riparian zones or wetlands. During the daytime, plant transpiration makes the groundwater table lower, and at night, the intensity of plant transpiration decreases and a significant rebound of the groundwater table level occurs. Based on the discovery of this pattern, White [81] proposed a classic method for calculating groundwater evapotranspiration, namely the White method. This method has long been used for groundwater evapotranspiration rates in arid and semi-arid areas [83,88–90]; it has been continuously improved by many researchers and has been applied to wetlands [8], riparian zones [79,91–93], prairies [94], and forests [95] in a variety of ecosystems.

### 2.2.1. White Method

The White method is the most classic method of the water-table fluctuation methods. White theorized that groundwater evapotranspiration is mainly composed of two parts—the recovery, and the storage variation in 24 h—based on the regular fluctuation of groundwater, which can be calculated by the following equation.

$$ET_g = S_y(24r \pm s) \quad (3)$$

where  $S_y$  is the specific yield of the shallow aquifer,  $r$  is the groundwater recharge rate from 00:00 a.m. to 04:00 a.m., and  $s$  is the 24-h shallow groundwater table variation. However, the White method is not universally applicable, and his application is based on four assumptions: (1) the day and night dynamics of groundwater table fluctuation are caused by plant evapotranspiration; (2) the evapotranspiration of plants from 0:00 a.m. to 4:00 a.m. at night is 0; (3) the groundwater recovery rate at night is a constant value; and (4) the specific

yield is a constant value and representative. Due to the simplicity and ease of operation of White method, this method is also the most widely used for evapotranspiration calculation at the site scale. However, some of the elements in the assumptions are subjective and limited, and researchers have made corresponding improvements in subsequent studies based on the shortcomings of the assumptions of the White method. Inspired by White method, many researchers have proposed other methods based on water-table fluctuation information, including the Dolan method [96], the Hays method [13], the Gribovski method [85], the Loheide method [62], the Soyulu method [86], etc. These methods are based on the White method and classed as approaches that improve upon the White method (Figure 1).

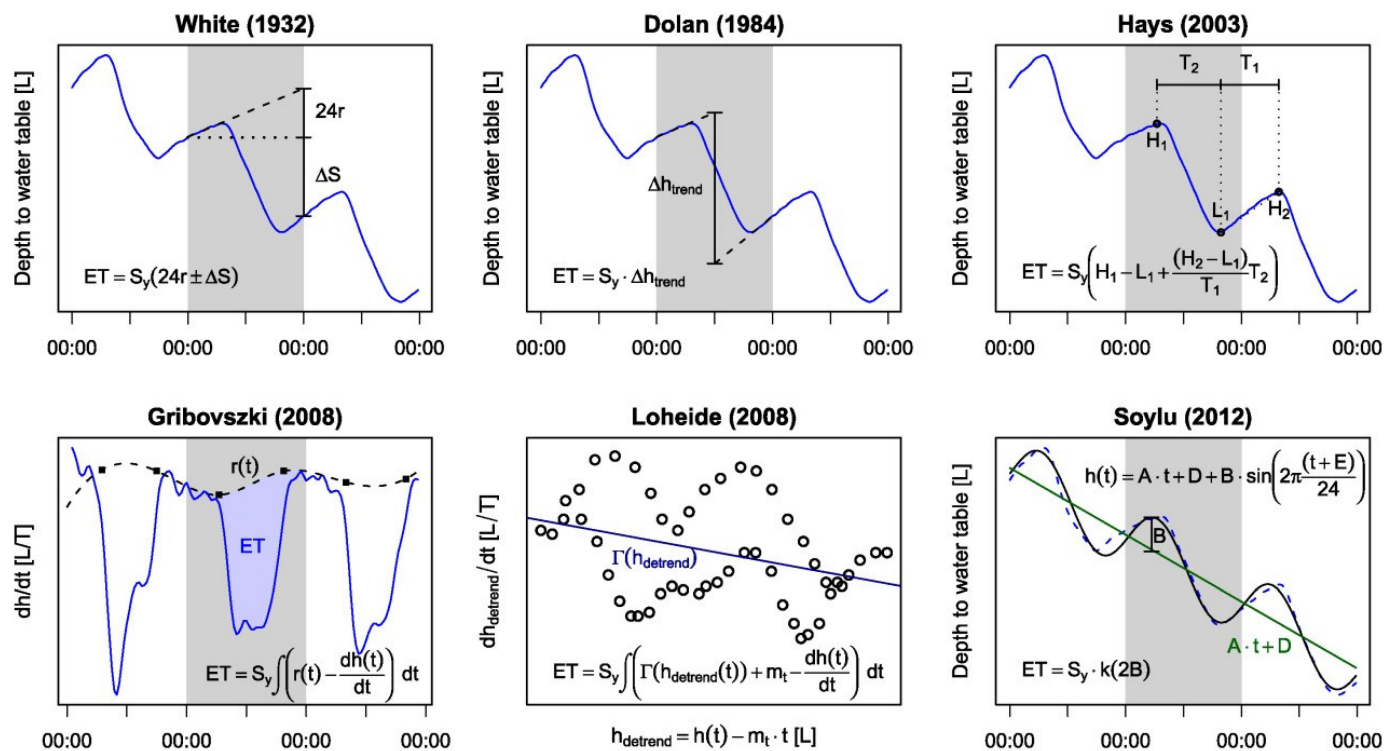


Figure 1. Computational schematic of the White method and its improved approaches [88].

### 2.2.2. Dolan Method

Dolan et al. [96] utilized continuous records of water-table elevation in the marsh soil, and related a drop in the water table to evapotranspiration loss. The observed rise or fall in the groundwater table at night represents the net inflow or outflow of water into or out of the marsh due to hydraulic forces alone. The rate of change of each night's groundwater table rise was extrapolated to noon the next day and back to noon the day before. The midday elevation represents the altitude of the groundwater table if no evapotranspiration had occurred during the 24 h period. The cycle is centered on each successive night. Thus, the difference between the elevation extrapolated from the previous night and the elevation extrapolated from the next night represents the water loss due to evapotranspiration on that day.

### 2.2.3. Hays Method

Hays [97] developed a new method for estimating  $ET_g$ . The biggest advantage of this method is the flexibility to determine the time of the water-table rise and fall according to the water-table waveform, instead of fixing it at a certain definite time period. Its calculation equation is:

$$ET_g = [(H_1 - H_L) + \frac{H_2 - H_L}{T_1} T_2] \times S_y \quad (4)$$



where  $H_1$  is the maximum water table depth on the morning of the calculation day in m,  $H_2$  is the maximum water table depth on the next day in m,  $H_L$  is the minimum water table depth on the day of the calculation in m,  $T_2$  is the duration of the groundwater table decline period, and  $T_1$  is the duration of the groundwater table rise period. The prerequisites for the use of the Hays method are similar to those of the White method.

#### 2.2.4. Loheide Method

The Loheide method [62] is an improved method based on the White method. The main idea of the Loheide method is that it is first assumed that the trend of the water table change in the recharge source is consistent with the general trend of observed water table change, so that the measured groundwater table can be detrended. The detrending analysis of the water table included in this method not only improves the calculation accuracy of vegetation evapotranspiration, but also reduces the uncertainty in the calculation process. The change in groundwater storage near the water table observation wells is expressed as the change in water table with time ( $dWT/dt$ ) and is controlled by the net inflow or outflow of groundwater in the vicinity ( $r(t)(L/T)$ ) together with the  $ET_g$ .

$$S_y^* \frac{dWT}{dt} = r(t) - ET_g(t) \quad (5)$$

When  $ET_g$  is 0, Equation (3) can be simplified as

$$S_y^* \frac{dWT}{dt} = r(t) \quad (6)$$

It has been clarified that the daily recharge rate is a function of time, and Loheide [52] assumes a constant head in the recharge source area and that the recharge rate can be obtained from water table changes, so Equation (5) can be expressed as

$$r(WT) = S_y^* \frac{dWT}{dt} \quad (7)$$

The Loheide method considers the trend of the groundwater recharge zone water table to be included in the water table change at the observation point, so this trend is therefore removed from the water table change at the observation point.

$$WT_{DT}(t) = WT(t) - m_T \times t - b_T \quad (8)$$

where  $WT_{DT}(t)$  is the detrended water table,  $WT(t)$  is the observed water table,  $m_T$  is the trend line slope, and  $b_T$  is the trend line intercept.  $dWT_{DT}/dt$  and  $WT_{DT}(t)$  using the water table of  $ET_g$  as 0 in the early morning of the current day and the next day, established the functional relationship  $\Gamma(WT_{DT})$ , and thus the recharge rate function is obtained, which can be expressed as

$$r(t) = S_y^* \times [\Gamma(WT_{DT}(t)) + m_T] \quad (9)$$

Finally, the available  $ET_g$  is expressed as:

$$ET_g(t) = r(t) - S_y^* \times \frac{dWT}{dt} \quad (10)$$

$S_y^*$  in the above equation is the complete specific yield instead of the traditional specific yield concept. The reason for the proposed concept of complete specific yield is because Loheide [62] theorized that the error of specific yield is an important factor in causing the error in the calculation of groundwater evapotranspiration. Therefore, he

proposed the concept of complete specific yield, and the equation of complete specific yield is as follows

$$S_y^* = S_{yu} - \frac{S_{yu}}{\left[1 + \alpha \left(\frac{z_i + z_f}{2}\right)^n\right]^{1 - \frac{1}{n}}}, S_{yu} = \theta_s - \theta_r \quad (11)$$

where  $\theta_s$  is the saturated soil water content,  $\theta_r$  is the residual water content, and  $z_i$  and  $z_f$  are the initial and end values for the variation of groundwater table depth. The parameters  $\alpha$  and  $n$  are in the van Genuchten model. The average values are taken when the groundwater table varies in the soil layer.

#### 2.2.5. Yin Method

The Loheide method assumes that the rate of change of the detrended water table is linearly related to the detrended water table. In response to this assumption, Yin et al. [12] further refined the Loheide method in their study, and found that applying the exponential equation to fit the relationship curve between the rate of change of the detrended water table and the detrended water table, can yield more accurate calculation results. Inspired by the Loheide method, Yin et al. [12] proposed an improved calculation of hourly-scale evapotranspiration based on the White method, as Equation (12)

$$ET_g = S_y \times (r + (H_{i-1} - H_i)) \quad (12)$$

where  $S_y$  is the specific yield,  $r$  is the water level recovery rate ( $LT^{-1}$ ),  $i$  is the moment value (T), and  $H$  is the water table value at the  $i^{th}$  moment (T). Compared with the Loheide method, the calculation process of this method is simpler.

#### 2.2.6. Gribovszki Method

Gribovszki et al. [85] also concluded that the rate of water table recovery is not constant throughout the day and proposed the use of empirical interpolation methods to calculate a non-constant rate of water table recovery throughout the day. The main idea is to estimate the rate by using hydraulic derivation and empirical methods. The maximum (positive) rate of water table changes between midnight and 6 a.m. and the average of  $dh/dt$  are chosen to obtain the maximum and minimum recharge rates, respectively. These values were assigned to the times of maximum and minimum groundwater table rates of recovery, respectively. Therefore, two points (sections) were defined for each day. Based on the points for several days, a spline interpolation was performed to describe the recharge rate  $r(t)$  (L/T) over time. Subdaily evapotranspiration was then calculated (e.g.,  $dt = 1$  h).

$$ET(t) = S_y \left( r(t) - \frac{dh}{dt} \right) \quad (13)$$

However, although the empirical interpolation method obtains the variation of water table recovery rate for each hour of the day, there may be some error in calculating the hour-by-hour water level recovery rate because the empirical interpolation method is based on only two pieces of daily data.

#### 2.2.7. Soyly Method

Soyly et al. [86] proposed to use a new 'Fourier method' to calculate groundwater evapotranspiration. They found that the amplitude of the fluctuations of the water table after detrending can be used to calculate evapotranspiration directly by combining the water balance equation of the White method and the Fourier equation proposed by Czikowsky and Fitzjarrald [98]. The equations are as follows.

$$H(t) = A \times t + D + B \sin \left( 2\pi \frac{(t + E)}{24} \right) \quad (14)$$

$$ET_g = S_y \times k(2B) \quad (15)$$

where  $H$  is the water table depth (L),  $A$  is the water table depth change trend for multiple days ( $LT^{-1}$ ),  $t$  is the time (T);  $D$  is the average deviation of water table depth change (L),  $B$  is the diurnal fluctuation amplitude (L),  $E$  is the day and night fluctuation phase (T), and  $k$  is the empirical correction factor for correcting the water table recovery and evapotranspiration components included in  $A \times t$ .

#### 2.2.8. Wang Method

Wang et al. [13] used the statistical method of day and night fluctuations of the water table to analyze the characteristics of de-trended groundwater table fluctuations, and then calculated the evapotranspiration at different time scales based on the relevant parameters. This method can effectively deal with continuously changing groundwater table fluctuation data.

$$ET_g = Sy \times \frac{\sigma}{\lambda} \quad (16)$$

where  $\sigma$  is the variance (L) of the variation of the de-trended water table, and  $\lambda$  is the evapotranspiration cycle correlation coefficient. It can be seen that the subsequent improvements in the water table fluctuation methods—both the Fourier method and the water table statistics method—are mostly improvements in the fluctuation characteristics about the detrended water table, and this series of improvement ideas is derived from the detrending theory proposed by Loheide.

#### 2.2.9. Other Improvements and Applications

Wang et al. [99] concluded that one of the limitations of the White method is the large uncertainty in quantifying the daily groundwater recovery rate ( $r$ ). Since  $ET_g$  is highly dependent on the shape and duration of the diurnal clear-sky solar radiation curve, using the groundwater recovery rate at short nighttime intervals to represent daily  $r$  may lead to large uncertainties in the  $ET_g$  estimates. They analyzed the dependence of the estimated daily  $r$  on sunset and sunrise times, and found that the estimated  $r$  is highly sensitive to the duration between sunset and sunrise and varies with the season. Instead of using fixed time spans ( $TS_s$ ), they suggest using a more universal method for determining  $TS_s$  for estimating daily  $r$ . They tested this dynamic T of S method at a *Tamarix ramosissima*-dominated riparian site in northwestern China. The results proved that their improved method was better and less subjective than the traditional White method. Subsequently, many researchers have used these representative methods mentioned above in different study areas for comparison to see their applicability. Three water table fluctuation methods [13,69,74] were used by Su et al. [100] in 2017 to calculate daily  $ET_g$  in a riparian forest area in northwestern China. The purpose of comparing these three methods was to evaluate and compare their performance under various groundwater table conditions in the wild. The results indicated that the White method is applicable to the period of declining groundwater table. In addition, the selected time period may affect the estimation of  $ET_g$ . The Soylu and Hays methods performed well under various groundwater table conditions. Therefore, it appears that the Hays and Soylu methods are more suitable for long-term  $ET_g$  estimation in the wild. In addition, it was found that the percentage of water transpired by plants from groundwater varies during the growing season, and that riparian plants mainly use soil water in early growth and tend to use groundwater in late growth. Yin et al. [12] also compared three frequently used water table fluctuation methods: the White, Hayes, and Loheide methods. These three methods use the water table generated by the model to calculate the  $ET_g$ . The comparison of actual and estimated  $ET_g$  reveals the accuracy of each method and determines the applicability of the methods. When the recovery branch of the groundwater table process line is nonlinear, these methods underestimate daily  $ET_g$ . The Loheide method is relatively good, and all three methods can accurately estimate daily  $ET_g$ . The modified White method can provide hourly  $ET_g$  estimates and is recommended for general use. It was found that in practical applications, analysis of the shape of the groundwater table recovery branch and the difference in groundwater head between the upper and lower gradients can determine the appropriate estimation method



of  $ET_g$ . Fahle and Dietrich [101] compared the existing water table fluctuation method with their field measurements of evapotranspiration. They used 85 days of rain-free data from a weighable groundwater solution meter located in the wetland meadows of the Spreewald in northeastern Germany. It can be shown that some researchers have used multiple water table fluctuation methods in different study areas around the world and have continuously made targeted improvements. These case studies continue to promote the development and improvement of water table fluctuation methods.

However, there are still some uncertainties regarding the White method and its improvements [102]. These uncertainties are mainly in the quantification of specific yield ( $S_y$ ), the choice of recharge time, the high heterogeneity of surface vegetation, and the effect of rainfall or irrigation on the water table. The largest uncertainty of White method mainly lies in the estimation of the  $S_y$ . The  $S_y$  was defined as the volume of water released by gravity from a unit area of rock column extending from the water table to the ground surface as the water table decreases by one unit depth (head) [103]. Errors in the  $S_y$  estimates translate directly into  $ET_g$  estimates [62,69,70,104]; both variables are involved in the  $ET_g$  calculation in the White method, since storage variability and groundwater recharge variability need to be multiplied by the  $S_y$ . However, there are many difficulties in estimating  $S_y$ , as this parameter is not constant over time. The specific yield is highly variable in shallow aquifers, and its magnitude depends on factors such as soil texture, water table depth, and the state of drainage or recharge [42,62,70,85,103,105–107].  $S_y$  is usually used only for groundwater drainage, but for rising water table conditions, the presence of air within the pore space is likely to reduce the value of  $S_y$ , i.e., the equivalent change in water table corresponds to a different change in water volume for the recharge and drainage states [42].

In addition, the White method for calculating the recharge rate (the underlying assumption for  $r$ ) uses the average rate of groundwater table rise between 0:00 a.m. and 04:00 a.m. for a total of 4 h to equal the average groundwater recharge rate for the entire day (Table 1); therefore, this method is not applicable to variable groundwater fluctuations. The recharge rate is typically a function of the head difference between the observation well and the recharge source [62]. The transient recharge rate will vary with time. Replacing the average daily recharge rate with the average daily recharge rate determined over a range of time can cause errors in the estimation of  $ET_g$  [106]. Therefore, many researchers usually modify the White method according to the time period used for recharge estimation [62,94,108]. Some other methods even avoid using varying recharge rates [13,86].

**Table 1.** The time periods selected for water table recovery rate calculation in different studies.

Method	Experimental Period
White [81]	0:00~4:00
Dolan et al. [96]	0:00~4:00
Hays [97]	0:00~4:00
Loheide [62]	0:00~6:00
Yin et al. [12]	the previous day 21:00~5:00
Rushton [108]	the previous day 18:00~6:00
Miller et al. [94]	the previous day 22:00~7:00

In addition to the degree of water availability and the timing of recharge, the magnitude of  $ET_g$  is also influenced by surface vegetation cover and the growth state of vegetation [109–111]. Of course, vegetation effects are not limited to groundwater evapotranspiration  $ET_g$ ; for total surface evapotranspiration  $ET$ , the contribution of plant transpiration ( $T$ ) to evapotranspiration ( $T/ET$ ) is estimated to range from 38 to 77% at the global scale, with an average of  $64 \pm 13\%$  [112–114]. Thus, terrestrial vegetation is an important force in the global water cycle [115]. In arid areas or areas with a low leaf area index (LAI), the average contribution of  $T$  to  $ET$  can reach 70% to 95% [113,116,117]. In arid or semi-arid zones, plants can only extract water from deeper soils or directly from the shallow water table for transpiration during the growing season due to the low water content of the topsoil.

Multiple indications suggest a strong correlation between the distribution of plant species and the depth of the groundwater table [118,119]. Vegetation has a strong adaptive capacity, especially in water-scarce ecosystems, to make full use of water in the unsaturated zone and aquifers through root growth [120,121]. Nepstad et al. [122] suggest that the semi-enclosed forests of the Brazilian Amazon rely on deep root systems to maintain a green canopy during the dry season. Evergreen forests can meet evapotranspiration requirements during droughts of up to 5 months by absorbing water from the soil at depths greater than 8 m. Maraun and Lafolie [123] found, in a maize-sorghum field in Nicaragua, that upward infiltration of water fluxes into the root zone reached 2 mm per day during drought, while actual evapotranspiration ranged from 2 to 4 mm per day. Kleidon and Heimann [124] similarly found that water uptake from deep soil or groundwater plays an important role in dry season transpiration in Amazonia. More recently, Saleska et al. [125] used Moderate Resolution Imaging Spectroradiometer (MODIS) satellite data to find that the greenness of Amazonian forests increased even during the 2005 drought, and concluded that trees were able to use deep roots to access groundwater to survive extreme drought periods. Considering the influence of crop growth processes on  $ET_g$ , Liu and Luo [126] combined two different methods, proposed by Doorenbos and Pruitt [59] and Schmid et al. [127], to calculate the values of groundwater evapotranspiration in areas with burial depths of less than 1.5 m for rainy periods (presence of rainfall or irrigation) and non-rainy periods, respectively. This method used a negative linear relationship between the water content of the unsaturated zone (root zone) and  $ET_g$ . However, when the groundwater depth is greater than 1.5 m, the variation in  $ET_g$  and the effect of irrigation can cause the relationship to deviate from the linear relationship. Under field conditions, the calculation of  $ET_g$  is influenced by multiple factors. Even during non-rainy periods (when there is no rainfall or irrigation)  $ET_g$  is still affected by multiple factors such as soil properties, crop water requirements, available soil water content, and groundwater table depth [128]. During rainy periods, a mixed upward and downward water potential gradient is formed in the soil profile [126], and downward fluxes caused by rainfall or irrigation may lead to a gradual development of local downward water potential gradients toward the bottom of the root zone. Some researchers, such as Yuan et al. [129], observed a significant positive correlation between evapotranspiration  $ET_g$  and potential evapotranspiration (PET). In addition, the results of Carlson Mazur [58] recognized a significant positive correlation between the two. Some studies have also reported that  $ET_g$  and potential PET have a weak positive correlation. According to some previous calculations, the  $R^2$  range of  $ET_g$  and PET was 0.02–0.43 [130]. Lautz [79] also reported a similar correlation between groundwater evapotranspiration ( $ET_g$ ) and potential evapotranspiration (PET) in semi-arid riverfront areas. Zhang et al. [131] reported that the strength of the correlation between  $ET_g$  and PET was significantly different in different research regions or conditions. The above complexity of the relationship between PET and  $ET_g$  is mainly due to their different controlling factors. Compared with PET, which is affected by climate conditions, there are many influencing factors for groundwater evapotranspiration, including plant species in the study area, root depth, local meteorological conditions, groundwater level variation patterns, lateral recharge and discharge of groundwater, and so on. Under the combined effect of these factors, groundwater evapotranspiration exhibits a large spatial and temporal heterogeneity.

The water table fluctuation (WTF) method, as a typical point-scale  $ET_g$  calculation method, is not a good choice in solving problems in terms of spatial heterogeneity. Due to some restrictive nature of its own application conditions and influenced by the uncertainty of the envelope, many researchers use numerical models as an auxiliary method to the water table fluctuation method to solve the problems of envelope uncertainty and spatial heterogeneity. Using an arid desert environment in northwestern China as his study area, Wang et al. [13] found that groundwater evapotranspiration is an important factor controlling hydrological processes in arid riparian zones, while the accuracy of estimating groundwater evapotranspiration values is influenced by the groundwater flow rate in the

aquifer, the redistribution of water within the riparian aquifer during river flow [132], and the specific yield [84]. He also used HYDRUS as a complement to understand the different seasonal variations in groundwater evapotranspiration values, but the point-scale HYDRUS+WTF approach still cannot address the uncertainties associated with time-varying lateral flow velocities, spatial variations in groundwater dynamic patterns, and specific yields in the riparian corridor, and he argued that monitoring networks rather than individual monitoring of point settings is necessary. Jia et al. [133] also used HYDRUS as a complement to the WTF method and found that in areas with shallow groundwater depths (<1 m), the groundwater replenishment of ET-induced depleted soils during nighttime is significant, and the use of the traditional White method would seriously underestimate groundwater evapotranspiration values because this factor is neglected; he therefore used HYDRUS to correct the omission of White method and used an improved method to estimate  $ET_g$ . Diouf et al. [134] also used HYDRUS and they found that in urban or shallow depth groundwater areas with agricultural irrigation, groundwater table fluctuation methods may be influenced by urban water use or agricultural irrigation, so in order to analyze the applicability of the WTF method to this area, he found that the WTF method achieved better accuracy in the evapotranspiration values calculated in the dry season using the water table simulated by HYDRUS; however, the accuracy was not guaranteed for different surfaces. The accuracy could be guaranteed only under the vegetation type. Therefore, the feasibility of using the simulation results of the numerical model as the source data for the WTF method to calculate the evapotranspiration needs to be further demonstrated. By studying historical data on water content and pressure level fluctuations on soil profiles. Zhao et al. [135] found that in a study area in northwest China, direct groundwater recharge does not occur from mid-June to mid-September when evapotranspiration is high, and soil water content changes in the upper unsaturated zone are mainly controlled by atmospheric conditions; however, in deeper parts, they are controlled by pressure surface fluctuations. Accordingly, a one-dimensional model (HYDRUS-1D) with variable head for the lower boundary condition (BC) was developed to explain the response of groundwater flow to changes in atmospheric and groundwater conditions, and the lower BC model with variable head reproduced the observed variation in soil moisture content, with a much smaller total evapotranspiration value obtained for the variable head below BC compared with the fixed head corresponding to the mean water table depth, which is similar to Zhu et al.'s model results [136].

### 2.3. Using the Numerical Model to Calculate the Groundwater Evapotranspiration

Unlike HYDRUS, another commonly used groundwater flow numerical model, MODFLOW [137], is often used without the need to incorporate the WTF method because it has a well-established  $ET_g$  calculation package. The calculation of  $ET_g$  is based on the fact that potential evapotranspiration shows a linear variation depending on the depth of the water table, with  $ET_g$  reaching a maximum when the water table is near the surface [138]. When the water table is below a fixed depth (ultimate evapotranspiration depth),  $ET_g$  is zero. In addition, MODFLOW includes the segmented linear evapotranspiration (ETS) package, which considers the segmented linear relationship between the depth of groundwater burial and the  $ET_g$  rate [138], and the ETS package more accurately represents the numerical variation of  $ET_g$  at different burial depth stages [139]. In the ETS package, the relation of ET rate to head is conceptualized as a segmented line (a piecewise linear function) in the variable interval. The segments that determine the shape of the function in the variable interval are defined by intermediate points where adjacent segments join. The ends of the segments at the top and bottom of the variable interval are defined by the ET surface and the extinction depth. For the simplest case, where a single ET segment is used (equivalent to the EVT package in MODFLOW2005), the ET rate is calculated as:

$$RET_{nb} = EVTR_{nb}, h_n > SURF_{nb} \quad (17)$$

$$RET_{nb} = EVTR_{nb} \frac{h_n - (SURF_{nb} - EXDP_{nb})}{EXDP_{nb}}, (SURF_{nb} - EXDP_{nb}) \leq h_n \leq SURF_{nb} \quad (18)$$

$$RET_{nb} = 0, h_n < (SURF_{nb} - EXDP_{nb}) \quad (19)$$

where  $RET_{nb}$  is the rate of loss per unit surface area of water table due to ET, in units of volume of water per unit area per unit time ( $LT^{-1}$ );  $h_n$  is the head, or water-table elevation in cell  $n$  from which the ET occurs (L);  $EVTR_{nb}$  is the maximum possible value of RET ( $LT^{-1}$ );  $SURF_{nb}$  is the ET surface elevation, or the water table elevation at which this maximum value of ET loss occurs (L); and  $EXDP_{nb}$  is the cutoff or extinction depth (L), such that when the distance between  $h_n$  and  $SURF_{nb}$  exceeds  $EXDP_{nb}$ , ET ceases.

Although the ETS package is an improvement in computational accuracy over the traditional EVT package, the calculations of the ETS package ignore other influences on  $ET_g$ , such as plant canopy cover, leaf area, community composition, and water content in the air pocket.

Pozdniakov et al. [140] argues that groundwater vapor emission has an important influence on the water balance in river valley zones, and he uses MODFLOW with the RIV and EVT packages to calculate  $ET_g$ . Based on the MODFLOW evapotranspiration package (EVT), Baird and Maddock [141] developed the Riparian Evapotranspiration for MODFLOW (RIP-ET) package to simulate riparian and wetland  $ET_g$  using a nonlinear  $ET_g$  curve that accounts for reduced  $ET_g$  rates due to hypoxic conditions. The spatial and temporal variability of riparian  $ET_g$  is controlled by climate, vegetation structure, water content of the unsaturated zone, and groundwater table depth (DTWT). To address the spatial heterogeneity of riparian zone vegetation  $ET_g$ , Ajami et al. [142] implemented a GIS tool in conjunction with RIPGIS-NET, which creates data input files in the MODFLOW-2000 or RIP-ET packages and visualizes MODFLOW results. Combining RIP-ET in MODFLOW with the GIS functionality of RIPGIS-NET can be used to calculate  $ET_g$  at different scales. This relationship was later modified in the evapotranspiration (ETS1) package to a segmented linear relationship, to include the nonlinearity between DTWT and  $ET_g$  rates. El-Zehairy et al. [143] calculated groundwater evapotranspiration  $ET_g$  and unsaturated zone evapotranspiration  $ET_{uz}$  for reservoir areas with large stage fluctuations in the water table by using MODFLOW with the addition of the packages SFR7, UZF1, and LAK7. Sergey et al. [144] analyzed the role of groundwater evapotranspiration in the water balance by using the MODFLOW-2005 hydrogeological model with the STR package; the annual variation of recharge was obtained with the codes from SurfBal and HYDRUS. The program code SurfBal is a surface water balance model, which was developed to simulate the processes of precipitation and heat energy transformations on the land surface in order to generate the upper boundary meteorological conditions for HYDRUS. Hou et al. [145] used the remote sensing evapotranspiration data ETwatch with the UZF1 package and MODFLOW to calculate the region-scale  $ET_g$  of the shallow depth groundwater zone in the eastern North China Plain.

Some other numerical models have also become common in recent years to calculate groundwater evaporation  $ET_g$ . Researchers conducting climate simulations have also started to calculate groundwater evapotranspiration [146–157]. Other researchers have combined numerical simulations with experiments to estimate groundwater evapotranspiration from agricultural fields [69,158]. Blin et al. [159] used evapotranspiration (ET) from the Earth Engine Evapotranspiration Flux (EEFlux) tool as calibration data, then used Parameter Estimation Software (PEST) as a tool to calibrate  $ET_g$  from MODFLOW for an undeveloped basin located in the arid Chilean highlands. Liu et al. [160] proposed an alternative approach to estimate ET through the lower boundary of the root zone (<1.0 m depth). Askri et al. [161] developed the hydrological model OASIS-MOD to study the effects of irrigation management on groundwater table fluctuations and soil salinity. The model involves evapotranspiration processes in the unsaturated zone, crop transpiration, and groundwater evapotranspiration processes.

### 3. Conclusions

Based on the above discussion, it is evident that accurate estimation of groundwater evapotranspiration is still a challenging task at present. The progress and breakthroughs in the technical methods related to this problem are mainly focused on two directions; the first is based on the theory of the WTF method, for which further improvement of the key parameters is required (such as specific yield  $S_y$  and groundwater recovery rate, etc.) There are various methods for improving the accuracy of the parameters, such as using numerical models or measuring in sample fields with the help of various instruments. It should be noted that the improvement of accuracy should not be limited only to the methods of obtaining parameters, and the discovery of new computational theories should not be ignored. The second type of method to calculate  $ET_g$  mainly relies on the numerical groundwater model. The distributed groundwater model can better solve the problem of spatial heterogeneity, and remote sensing technology can provide more accurate hydrological and meteorological parameters for the model, but the uncertainty of the unsaturated zone blocks the combination of remote sensing technology and the groundwater model, so the coupled model of surface remote sensing data and the unsaturated zone model and groundwater model, should subsequently be constructed for calculating the groundwater evapotranspiration at a regional scale.

**Author Contributions:** Writing—original draft, X.H.; writing—review and editing, H.Y. and J.C.; conceptualization, W.F. and Y.Z. All authors have read and agreed to the published version of the manuscript.

**Funding:** This research was financially supported by the Science & Technology Fundamental Resources Investigation Program (grant numbers 2022FY100104), National Natural Science Foundation of China (grant number 42001009), the Key Research and Development Plan Project of Hebei Province (grant numbers 20324201D, 22324202D, 20536001D), the Open Project of Water Environment Science Laboratory in Hebei Province, China (grant number HBSHJ202101) and the Science and Technology Program of Hebei Academy of Sciences, China (22106).

**Institutional Review Board Statement:** Not applicable.

**Informed Consent Statement:** Not applicable.

**Data Availability Statement:** All data, models, and code generated or used during the study appear in the submitted article.

**Conflicts of Interest:** The authors declare no conflict of interest.

### References

1. Xue, J.Y.; Guan, H.D.; Huo, Z.L.; Wang, F.X.; Huang, G.H.; Boll, J. Water saving practices enhance regional efficiency of water consumption and water productivity in an arid agricultural area with shallow groundwater. *Agric. Water Manag.* **2017**, *194*, 78–89. [CrossRef]
2. Rijsberman, F.R. Water scarcity: Fact or fiction? *Agric. Water Manag.* **2006**, *80*, 5–22. [CrossRef]
3. Vörösmarty, C.J.; Green, P.; Salisbury, J.; Lammers, R. Global water resources: vulnerability from climate change and population growth. *Science* **2000**, *289*, 284–288. [CrossRef]
4. Yeh, P.J.F.; Famiglietti, J.S. Regional groundwater evapotranspiration in Illinois. *J. Hydrometeorol.* **2009**, *10*, 464–478. [CrossRef]
5. Babajimopoulos, C.; Panoras, A.; Georgoussis, H.; Arampatzis, G.; Hatzigiannakis, E.; Papamichail, D. Contribution to irrigation from shallow water table under field conditions. *Agric. Water Manag.* **2007**, *92*, 205–210. [CrossRef]
6. Dregne, H.E. Global status of desertification. *Ann. Arid Zone* **1991**, *30*, 179–185.
7. NOAA, JetStream: Online School for Weather. Available online: [http://www.srh.noaa.gov/jetstream/global/climate\\_max.htm](http://www.srh.noaa.gov/jetstream/global/climate_max.htm) (accessed on 26 February 2023).
8. Bulter, J.J., Jr.; Kluitenberg, G.J.; Whittemore, D.O.; Loheide, S.P., II; Jin, W.; Billinger, M.A.; Zhan, X.Y. A field investigation of phreatophyte-induced fluctuations in the water-table. *Water Resources Res.* **2007**, *43*, W02404.
9. Gribovszki, Z.; Szilágyi, J.; Kalicz, P. Diurnal fluctuations in shallow groundwater levels and streamflow rates and their interpretation—A review. *J. Hydrol.* **2010**, *385*, 371–383. [CrossRef]
10. Scanlon, B.R.; Keese, K.E.; Flint, A.L.; Flint, L.E.; Gaye, C.B.; Edmunds, W.M.; Simmers, I. Global synthesis of groundwater recharge in semiarid and arid regions. *Hydrol. Process.* **2006**, *20*, 3335–3370. [CrossRef]



11. Qi, S.Z.; Luo, F. Hydrological indicators of desertification in the Heihe River Basin of arid northwest China. *AMBIO A J. Hum. Environ.* **2006**, *35*, 319–321.
12. Yin, L.H.; Zhou, Y.X.; Ge, S.M.; Wen, D.G.; Zhang, E.Y.; Dong, J.Q. Comparison and modification of methods for estimating evapotranspiration using diurnal groundwater level fluctuations in arid and semiarid regions. *J. Hydrol.* **2013**, *496*, 9–16. [\[CrossRef\]](#)
13. Wang, P.; Grinevsky, S.O.; Pozdniakov, S.P. Application of the water table fluctuation method for estimating evapotranspiration at two phreatophyte-dominated sites under hyper-arid environments. *J. Hydrol.* **2014**, *519*, 2289–2300. [\[CrossRef\]](#)
14. Goodrich, D.C.; Scott, R.; Qi, J.; Goff, B.; Unkrich, C.L.; Moran, M.S.; Williams, D.; Schaeffer, S.; Snyder, R.K.; MacNish, R.; et al. Seasonal estimates of riparian evapotranspiration using remote and in situ measurements. *Agric. For. Meteorol.* **2000**, *105*, 281–309. [\[CrossRef\]](#)
15. Wang, X.W.; Huo, Z.L.; Feng, S.Y.; Guo, P.; Guan, H.D. Estimating groundwater evapotranspiration from irrigated cropland incorporating root zone soil texture and moisture dynamics. *J. Hydrol.* **2016**, *543*, 501–509. [\[CrossRef\]](#)
16. Drexler, J.Z.; Snyder, R.L.; Spano, D.; Tha Paw, U.K. A review of models and micrometeorological methods used to estimate wetland evapotranspiration. *Hydrol. Process.* **2004**, *18*, 2071–2101. [\[CrossRef\]](#)
17. Cooper, D.J.; Sanderson, J.S.; Stannard, D.I.; Groeneveld, D.P. Effects of long-term water table drawdown on evapotranspiration and vegetation in an arid region phreatophyte community. *J. Hydrol.* **2006**, *325*, 21–34. [\[CrossRef\]](#)
18. Naumburg, E.; Mata-Gonzalez, R.; Hunter, R.G.; McIendon, T.; Martin, D.W. Phreatophytic vegetation and groundwater fluctuations: A review of current research and application of ecosystem response modeling with an emphasis on great basin vegetation. *Environ. Manag.* **2005**, *35*, 726–740. [\[CrossRef\]](#)
19. Orellana, F.; Verma, P.; Loheide, S.P., II; Daly, E. Monitoring and modeling water-vegetation interactions in groundwater-dependent ecosystems. *Rev. Geophys.* **2012**, *50*, 3. [\[CrossRef\]](#)
20. Yuan, G.F.; Zhang, P.; Shao, M.A.; Luo, Y.; Zhu, X.C. Energy and water exchanges over a riparian Tamarix spp. stand in the lower Tarim River basin under a hyper-arid climate. *Agric. For. Meteorol.* **2014**, *194*, 144–154. [\[CrossRef\]](#)
21. Salama, R.B.; Fitzpatrick, O. Contributions of groundwater conditions to soil and water salinization. *Hydrogeol. J.* **1999**, *7*, 46–64. [\[CrossRef\]](#)
22. Northey, J.E.; Christen, E.W.; Ayars, J.E.; Jankowski, J. Occurrence and measurement of salinity stratification in shallow groundwater in the Murrumbidgee Irrigation Area, south-eastern Australia. *Agric. Water Manag.* **2006**, *81*, 23–40. [\[CrossRef\]](#)
23. Zipper, S.C.; Soyulu, M.E.; Booth, E.G.; Loheide, S.P., II. Untangling the effects of shallow groundwater and soil texture as drivers of subfield-scale yield variability. *Water Resour. Res.* **2015**, *51*, 6338–6358. [\[CrossRef\]](#)
24. Ayars, J.E.; Schoneman, R.A. Use of saline water from a shallow water table by cotton. *Trans ASAE* **1986**, *29*, 1674–1678. [\[CrossRef\]](#)
25. Yang, F.; Zhang, G.; Yin, X.; Liu, Z.; Huang, Z. Study on capillary rise from shallow groundwater and critical water table depth of a saline-sodic soil in western Songnen plain of China. *Environ. Earth Sci.* **2011**, *64*, 2119–2126. [\[CrossRef\]](#)
26. Pratharpar, S.A.; Qureshi, A.S. Modelling the effects of deficit irrigation on soil salinity, depth to water table and transpiration in semi-arid zones with monsoonal rains. *Int. J. Water Resour. Dev.* **1999**, *15*, 141–159. [\[CrossRef\]](#)
27. Yang, J.F.; Li, B.Q.; Liu, S.P. A large weighing lysimeter for evapotranspiration and soil-water-groundwater exchange studies. *Hydrol. Process.* **2000**, *14*, 1887–1897. [\[CrossRef\]](#)
28. Kahlow, M.A.; Ashraf, M. Zia-ul-Haq, Effect of shallow groundwater table on crop water requirements and crop yields. *Agric. Water Manag.* **2005**, *76*, 24–35. [\[CrossRef\]](#)
29. Wu, Y.; Liu, T.; Paredes, P.; Duan, L.; Pereira, L.S. Water use by a groundwater dependent maize in a semi-arid region of Inner Mongolia: Evapotranspiration partitioning and capillary rise. *Agric. Water Manag.* **2015**, *152*, 222–232. [\[CrossRef\]](#)
30. Gou, S.; Miller, G. A groundwater-soil-plant-atmosphere continuum approach for modelling water stress, uptake, and hydraulic redistribution in phreatophytic vegetation. *Ecohydrology* **2014**, *7*, 1029–1041. [\[CrossRef\]](#)
31. Newman, B.D.; Wilcox, B.P.; Archer, S.R.; Breshears, D.D.; Dahm, C.N.; Duffy, C.J.; McDowell, N.G.; Phillips, F.M.; Scanlon, B.R.; Vivoni, E.R. Ecohydrology of water-limited environments: A scientific vision. *Water Resour. Res.* **2006**, *42*, W06302. [\[CrossRef\]](#)
32. Allen, R.G. Assessing integrity of weather data for reference evapotranspiration estimation. *J. Irrig. Drain. Eng.* **1996**, *122*, 97–106. [\[CrossRef\]](#)
33. Balugani, E.; Lubczynski, M.W.; Reyes-Acosta, L.; Van Der, T.C.; Francés, A.P.; Metselaar, K. Groundwater and unsaturated zone evaporation and transpiration in a semi-arid open wood land. *J. Hydrol.* **2017**, *547*, 54–66. [\[CrossRef\]](#)
34. Lubczynski, M.W.; Gurwin, J. Integration of various data sources for transient groundwater modeling with spatio-temporally variable fluxes—Sardon study case, Spain. *J. Hydrol.* **2005**, *306*, 71–96. [\[CrossRef\]](#)
35. Gavilán, P.; Berengena, J.; Allen, R.G. Measuring versus estimating net radiation and soil heat flux: Impact on penman–monteith reference et estimates in semiarid regions. *Agric. Water Manag.* **2007**, *89*, 275–286. [\[CrossRef\]](#)
36. Gazal, R.M.; Scott, R.L.; Goodrich, D.C.; Williams, D.G. Controls on transpiration in a semiarid riparian cottonwood forest. *Agric. For. Meteorol.* **2006**, *137*, 56–67. [\[CrossRef\]](#)
37. Hultine, K.R.; Bush, S.E.; West, A.G.; Ehleringer, J.R. Effect of gender on sap-flux-scaled transpiration in a dominant riparian tree species: Box elder (acer negundo). *J. Geophys. Res. Biogeosci.* **2015**, *112*, 87–101. [\[CrossRef\]](#)
38. Moore, D.J.P.; Hu, J.; Sacks, W.J.; Schimel, D.S.; Monson, R.K. Estimating transpiration and the sensitivity of carbon uptake to water availability in a subalpine forest using a simple ecosystem process model informed by measured net CO<sub>2</sub> and H<sub>2</sub>O fluxes. *Agric. For. Meteorol.* **2008**, *148*, 1467–1477. [\[CrossRef\]](#)

39. Lenka, S.; Singh, A.K.; Lenka, N.K. Water and nitrogen interaction on soil profile water extraction and ET in maize-wheat cropping system. *Agric. Water Manag.* **2009**, *96*, 195–207. [\[CrossRef\]](#)
40. Richard, G.; Benyon, S.; Theiveyanathan Doody, T.M. Impacts of tree plantations on groundwater in south-eastern Australia. *Aust. J. Bot.* **2006**, *54*, 181–192.
41. Doody, T.; Benyon, R. Quantifying water savings from willow removal in Australian streams. *J. Environ. Manag.* **2011**, *92*, 926–935. [\[CrossRef\]](#)
42. Nachabe, M.; Shah, N.; Ross, M.; Vomacka, J. Evapotranspiration of two vegetation covers in a shallow water table environment. *Soil Sci. Soc. Am. J.* **2005**, *69*, 492–499. [\[CrossRef\]](#)
43. Devitt, D.A.; Fenstermaker, L.F.; Young, M.H.; Conrad, B.; Baghzouz, M.; Bird, B.M. Evapotranspiration of mixed shrub communities in phreatophytic zones of the Great Basin region of Nevada (USA). *Ecohydrology* **2011**, *4*, 807–822. [\[CrossRef\]](#)
44. Moore, G.W.; Cleverly, J.R.; Owens, M.K. Nocturnal transpiration in riparian Tamarix thickets authenticated by sap flux, eddy covariance and leaf gas exchange measurements. *Tree Physiol.* **2008**, *28*, 521–528. [\[CrossRef\]](#)
45. Scott, R.L.; Edwards, E.A.; Shuttleworth, W.J.; Huxman, T.E.; Watts, C.; Goodrich, D.C. Interannual and seasonal variation in fluxes of water and carbon dioxide from a riparian woodland ecosystem. *Agric. For. Meteorol.* **2004**, *122*, 65–84. [\[CrossRef\]](#)
46. Scott, R.L.; Huxman, T.E.; Williams, D.G.; Goodrich, D.C. Ecohydrological impacts of woody-plant encroachment: Seasonal patterns of water and carbon dioxide exchange within a semiarid riparian environment. *Glob. Change Biol.* **2006**, *12*, 311–324. [\[CrossRef\]](#)
47. Scott, R.L.; Shuttleworth, W.J.; Goodrich, D.C. The water use of two dominant vegetation communities in a semiarid riparian ecosystem. *Agric. For. Meteorol.* **2000**, *105*, 241–256. [\[CrossRef\]](#)
48. Norman, J.M.; Kustas, W.P.; Humes, K.S. Source approach for estimating soil and vegetation energy fluxes in observations of directional radiometric surface temperature. *Agric. For. Meteorol.* **1995**, *77*, 263–293. [\[CrossRef\]](#)
49. Bastiaanssen, W.G.M.; Pelgrum, H.; Wang, J.; Ma, Y.; Moreno, J.F.; Roerink, G.J.; van der Wal, T. A remote sensing surface energy balance algorithm for land (SEBAL): Part 2: Valiation. *J. Hydrol.* **1998**, *212*, 213–229. [\[CrossRef\]](#)
50. Roerink, G.J.; Su, Z.; Menenti, M. S-SEBI: A simple remote sensing algorithm to estimate the surface energy balance. *Phys. Chem. Earth Part B Hydrol. Oceans Atmos.* **2000**, *25*, 147–157. [\[CrossRef\]](#)
51. Su, Z. The surface energy balance system (SEBS) for estimation of turbulent heat fluxes. *Hydrol. Earth Syst. Sci.* **2002**, *6*, 85–99. [\[CrossRef\]](#)
52. Gellens-Meulenberghs, F.; Arboleda, A.; Ghilain, N. Towards a continuous monitoring of evapotranspiration based on MSG data. *Environ. Sci.* **2007**, *316*, 228–234.
53. Allen, R.G.; Tasumi, M.; Trezza, R. Satellite-based energy balance for mapping evapotranspiration with internalized calibration (METRIC)-model. *J. Irrigat. Drain. Eng.* **2007**, *133*, 380–394. [\[CrossRef\]](#)
54. Sánchez, J.M.; Kustas, W.P.; Caselles, V.; Anderson, M.C. Modelling surface energy fluxes over maize using a two-source patch model and radiometric soil and canopy temperature observations. *Remote Sens. Environ.* **2008**, *112*, 1130–1143. [\[CrossRef\]](#)
55. Miralles, D.G.; Holmes, T.R.H.; Dejeu, R.A.M.; Gash, J.H.; Meesters, A.G.C.A. Global land-surface evaporation estimated from satellite-based observations. *Hydrol. Earth Syst. Sci. Discuss.* **2011**, *7*, 453–469. [\[CrossRef\]](#)
56. Mu, Q.; Zhao, M.; Running, S.W. Improvements to a MODIS global terrestrial evapotranspiration algorithm. *Remote Sens. Environ.* **2011**, *115*, 1781–1800. [\[CrossRef\]](#)
57. Wu, B.F.; Yan, N.N.; Xiong, J.; Bastiaanssen, W.G.M.; Zhu, W.W.; Stein, A. Validation of ETWatch using field measurements at diverse landscapes: A case study in Hai basin of China. *J. Hydrol.* **2012**, *436*, 67–80. [\[CrossRef\]](#)
58. Mazur, M.C.; Wiley, M.J.; Wilcox, D.A. Estimating evapotranspiration and groundwater flow from water-table fluctuations for a general wetland scenario. *Ecohydrology* **2014**, *7*, 378–390. [\[CrossRef\]](#)
59. Ridolfi, L.; Odorico, P.D.; Laio, F. Vegetation dynamics induced by phreatophyte-aquifer interactions. *J. Theor. Biol.* **2007**, *248*, 301–310. [\[CrossRef\]](#)
60. Sanderson, J.S.; Cooper, D.J. Ground water discharge by evapotranspiration in wetlands of an arid intermountain basin. *J. Hydrol.* **2008**, *351*, 344–359. [\[CrossRef\]](#)
61. Healy, R.W.; Scanlon, B.R. *Estimating Groundwater Recharge: Groundwater Recharge*; Cambridge University Press: Cambridge, UK, 2010.
62. Loheide II, S.P. A method for estimating subdaily evapotranspiration of shallow groundwater using diurnal water table fluctuations. *Ecohydrology* **2008**, *1*, 59–66. [\[CrossRef\]](#)
63. Simmers, I.; Hendrickx, J.; Kruseman, G.P.; Rushton, K.R. *Recharge of Phreatic Aquifers in (Semi-) Arid Areas*; Balkema: Rotterdam, The Netherlands, 1997.
64. Yu, L.Y.; Zeng, Y.J.; Su, Z.B.; Cai, H.J.; Zheng, Z. The effect of different evapotranspiration methods on portraying soil water dynamics and ET partitioning in a semi-arid environment in Northwest China. *Hydrol. Earth Syst. Sci.* **2016**, *20*, 975–990. [\[CrossRef\]](#)
65. Remson, I.; Fox, G.S. Capillary losses from ground water. *Trans. Am. Geophys. Union* **1955**, *36*, 304–310. [\[CrossRef\]](#)
66. Gardner, W.R. Some steady-state solutions of the unsaturated moisture flow equation with application to evaporation from a water table. *Soil Sci.* **1958**, *85*, 228–232. [\[CrossRef\]](#)
67. Willis, W.O. Evaporation from layered soils in the presence of a water table. *Soil Sci. Soc. Am. J.* **1960**, *24*, 239–242. [\[CrossRef\]](#)
68. Schoeller, H. *Les Eaux Souterraines*; Mason and Cie: Paris, France, 1962; Volume 642.

69. Doorenbos, J.; Pruitt, W.O. *FAO Guidelines for Predicting Crop Water Requirements*; FAO Irrigation & Drainage Paper; Food and Agriculture Organization of the United Nations: Rome, Italy, 1975.
70. Steinwand, A.L.; Harrington, R.F.; Or, D. Water balance for great basin phreatophytes derived from eddy covariance, soil water, and water table measurements. *J. Hydrol.* **2006**, *329*, 595–605. [\[CrossRef\]](#)
71. Stuff, R.G.; Dale, R.F. A soil moisture budget model accounting for shallow water table influences. *Soil Sci. Soc. Am. J.* **1978**, *42*, 637–643. [\[CrossRef\]](#)
72. Wallender, W.W.; Grimes, D.W.; Henderson, D.W.; Stromberg, L.K. Estimating the contribution of a perched water table to the seasonal evapotranspiration of cotton. *Agron. J.* **1979**, *71*, 1056–1060. [\[CrossRef\]](#)
73. Loheide, S.P., II; Butler, J.J.; Gorelick, S.M. Estimation of groundwater consumption by phreatophytes using diurnal water table fluctuations: A saturated-unsaturated flow assessment. *Water Resour. Res.* **2005**, *41*, W07030. [\[CrossRef\]](#)
74. Wang, X.W.; Huo, Z.L.; Shukla, M.K.; Wang, X.H.; Guo, P.; Xu, X.; Huang, G.H. Energy fluxes and evapotranspiration over irrigated maize field in an arid area with shallow groundwater. *Agric. Water Manag.* **2020**, *228*, 105922. [\[CrossRef\]](#)
75. Ren, D.Y.; Xu, X.; Hao, Y.Y.; Huang, G.H. Modeling and assessing field irrigation water use in a canal system of Hetao, upper Yellow River basin: Application to maize, sunflower and watermelon. *J. Hydrol.* **2016**, *532*, 122–139. [\[CrossRef\]](#)
76. Lai, J.; Liu, T.; Luo, Y. Evapotranspiration Partitioning for Winter Wheat with Shallow Groundwater in the Lower Reach of the Yellow River Basin. *Agric. Water Manag.* **2022**, *266*, 107561. [\[CrossRef\]](#)
77. Karimov, A.K.; Šimůnek, J.; Hanjra, M.A.; Avliyakov, M.; Forkutsa, I. Effects of the shallow water table on water use of winter wheat and ecosystem health: Implications for unlocking the potential of groundwater in the Fergana Valley (Central Asia). *Agric. Water Manag.* **2014**, *131*, 57–69. [\[CrossRef\]](#)
78. Nirjhar, S.; Mahmood, N.; Mark, R. Extinction depth and evapotranspiration from ground water under selected land covers. *Ground Water* **2007**, *45*, 329–338.
79. Lautz, L.K. Estimating groundwater evapotranspiration rates using diurnal water-table fluctuations in a semi-arid riparian zone. *Hydrogeol. J.* **2008**, *16*, 483–497. [\[CrossRef\]](#)
80. Mould, D.J.; Frahm, E.; Salzmänn Th Miegel, K.; Acreman, M.C. Evaluating the use of diurnal groundwater fluctuations for estimating evapotranspiration in wetland environments: Case studies in southeast England and northeast Germany. *Ecology* **2010**, *3*, 294–305. [\[CrossRef\]](#)
81. White, W.N. *Method of Estimating Ground-Water Supplies Based on Discharge by Plants and Evaporation from Soil: Results of Investigation in Escalante Valley, Utah (R)*; Geological Survey Water Supply Paper, 659-A; United States Department of the Interior, Government Printing Office: Washington, DC, USA, 1932; Volume 115.
82. Meyboom, P. Three observations on streamflow depletion by phreatophytes. *J. Hydrol.* **1965**, *2*, 248–261. [\[CrossRef\]](#)
83. Gerla, P.J. The Relationship of Water-Table Changes to the Capillary Fringe, Evapotranspiration, and Precipitation in Intermittent Wetlands. *Wetlands* **1992**, *12*, 91–98. [\[CrossRef\]](#)
84. Healy, R.W.; Cook, P.G. Using groundwater levels to estimate recharge. *Hydrogeol. J.* **2002**, *10*, 91–109. [\[CrossRef\]](#)
85. Gribovszki, Z.; Kalicz, P.; Szilagyi, J.; Kucsara, M. Riparian zone evapotranspiration estimation from diurnal groundwater level fluctuations. *J. Hydrol.* **2008**, *349*, 6–17. [\[CrossRef\]](#)
86. Soylu, M.E.; Lenters, J.D.; Istanbuloglu, E.; Loheide, S.P., II. On evapotranspiration and shallow groundwater fluctuations: A fourier-based improvement to the white method. *Water Resources Res.* **2012**, *48*, W06506. [\[CrossRef\]](#)
87. Wang, P.; Yu, J.J.; Pozdniakov, S.P.; Grinevsky, S.O.; Liu, C.M. Shallow groundwater dynamics and its driving forces in extremely arid areas: A case study of the lower Heihe river in northwestern China. *Hydrol. Process.* **2014**, *28*, 1539–1553. [\[CrossRef\]](#)
88. Troxell, H.C. The diurnal fluctuation in the ground-water and flow of the Santa Ana river and its meaning. *Trans. Am. Geophys. Union* **1936**, *17*, 496–504. [\[CrossRef\]](#)
89. Gatewood, J.S. Use of water by bottom-land vegetation in lower Safford valley, Arizona. *US Geol. Surv. Water Supply Pap.* **1950**, *1103*, 210.
90. Lacznak, R.J.; Demeo, G.A.; Reiner, S.R.; Smith, J.L.; Nylund, W.E. *Estimates of Ground-Water Discharge as Determined from Measurements of Evapotranspiration, Ash Meadows area, Nye County, Nevada*; USGS US Geological Survey Water Resources Investigations Report 99-4079; Geological Survey: Las Vegas, NV, USA, 1999.
91. McLaughlin, D.L.; Cohen, M.J. Ecosystem specific yield for estimating evapotranspiration and groundwater exchange from diel surface water variation. *Hydrol. Process.* **2013**, *28*, 1495–1506. [\[CrossRef\]](#)
92. Schilling, K.E. Water table fluctuations under three riparian land covers, Iowa (USA). *Hydrol. Process.* **2010**, *21*, 2415–2424. [\[CrossRef\]](#)
93. Martinet, M.C.; Vivoni, E.R.; Cleverly, J.R.; Thibault, J.R.; Dahm, C.N. On groundwater fluctuations, evapotranspiration, and understory removal in riparian corridors. *Water Resour. Res.* **2009**, *45*, 207–213. [\[CrossRef\]](#)
94. Miller, G.R.; Chen, X.; Rubin, Y.; Ma, S.; Baldocchi, D.D. Groundwater uptake by woody vegetation in a semiarid oak savanna. *Water Resour. Res.* **2010**, *46*, 2290–2296. [\[CrossRef\]](#)
95. Vincke, C.; Thiry, Y. Water table is a relevant source for water uptake by a Scots pine (*Pinus sylvestris* L.) stand: Evidence from continuous evapotranspiration and water table monitoring. *Agric. For. Meteorol.* **2008**, *148*, 1419–1432. [\[CrossRef\]](#)
96. Dolan, T.J.; Hermann, A.J.; Bayley, S.E.; Zoltek, J.J. Evapotranspiration of a Florida, U.S.A. freshwater wetland. *J. Hydrol.* **1984**, *74*, 355–371. [\[CrossRef\]](#)



97. Hays, K.B. Water Use by Saltcedar (*Tamarix* sp.) and Associated Vegetation on the Canadian, Colorado and Pecos Rivers in Texas. Master's Thesis, Texas A & M University, Texas, TX, USA, 2003.
98. Czikowsky, M.J.; Fitzjarrald, D.R. Evidence of seasonal changes in evapotranspiration in eastern u.s. hydrological records. *J. Hydrometeorol.* **2009**, *5*, 974–988. [\[CrossRef\]](#)
99. Wang, T.Y.; Wang, P.; Yu, J.J.; Pozdniakov, S.P.; Zhang, Y. Revisiting the white method for estimating groundwater evapotranspiration: A consideration of sunset and sunrise timings. *Environ. Earth Sci.* **2019**, *78*, 412.1–412.7. [\[CrossRef\]](#)
100. Su, Y.H.; Feng, Q.; Zhu, G.F.; Zhang, Q. Evaluating the different methods for estimating groundwater evapotranspiration using diurnal water table fluctuations. *J. Hydrol.* **2022**, *607*, 127508.
101. Fahle, M.; Dietrich, O. Estimation of evapotranspiration using diurnal groundwater level fluctuations: Comparison of different approaches with groundwater lysimeter data. *Water Resour. Res.* **2014**, *50*, 273–286. [\[CrossRef\]](#)
102. Acharya, S.; Jawitz, J.W.; Mylavarapu, R.S. Analytical expressions for drainable and fillable porosity of phreatic aquifers under vertical fluxes from evapotranspiration and recharge. *Water Resour. Res.* **2012**, *48*, W11526. [\[CrossRef\]](#)
103. Sophocleous, M. The role of specific yield in ground-water recharge estimations: A numerical study. *Groundwater* **1985**, *23*, 52–58. [\[CrossRef\]](#)
104. Cheng, D.H.; Li, Y.; Chen, X.; Wang, W.K.; Hou, G.C.; Wang, C.L. Estimation of groundwater evapotranspiration using diurnal water table fluctuations in the mu us desert, northern China. *J. Hydrol.* **2013**, *490*, 106–113. [\[CrossRef\]](#)
105. Duke, H.R. Capillary properties of soils—influence upon specific yield. *Amer Soc Agr Eng Trans Asae* **1972**, *15*, 688–691. [\[CrossRef\]](#)
106. Alley, W.M.; Healy, R.W.; Labaugh, J.W.; Reilly, T.E. Flow and storage in groundwater systems. *Science* **2002**, *296*, 1985–1990. [\[CrossRef\]](#)
107. Scanlon, B.R.; Faunt, C.C.; Longuevergne, L.; Reedy, R.C.; McMahon, P.B. Groundwater depletion and sustainability of irrigation in the us high plains and central valley. *Proc. Natl. Acad. Sci. USA* **2012**, *109*, 9320–9325. [\[CrossRef\]](#)
108. Rushton, B. Hydrologic budget for a freshwater marsh in Florida. *Water Resour. Bull.* **1996**, *32*, 13–21. [\[CrossRef\]](#)
109. Bethenod, O.; Katerji, N.; Goujet, R.; Bertolini, J.M.; Rana, G. Determination and validation of corn crop transpiration by sap flow measurement under field conditions. *Theor. Appl. Climatol.* **2000**, *67*, 153–160. [\[CrossRef\]](#)
110. Hsiao, B.T.; Xu, L. Evapotranspiration and Relative Contribution by the Soil and the Plant. *Calif. Water Plan Update* **2005**, *4*, 129–160.
111. Wilson, K.B.; Hanson, P.J.; Baldocchi, D.D. Factors controlling evaporation and energy partitioning beneath a deciduous forest over an annual cycle. *Agric. For. Meteorol.* **2000**, *102*, 83–103. [\[CrossRef\]](#)
112. Coenders-Gerrits, A.M.J.; van der Ent, R.J.; Bogaard, T.A.; Wang, E.L.; Harchowitz, M.; Savenijie, H.H.G. Uncertainties in transpiration estimates. *Nature* **2014**, *506*, E1–E2. [\[CrossRef\]](#)
113. Wang, L.; Good, S.P.; Caylor, K.K. Global synthesis of vegetation control on evapotranspiration partitioning. *Geophys. Res. Lett.* **2014**, *41*, 6753–6757. [\[CrossRef\]](#)
114. Good, S.P.; Noone, D.; Bowen, G. Hydrologic connectivity constrains partitioning of global terrestrial water fluxes. *Science* **2015**, *349*, 175–177. [\[CrossRef\]](#)
115. Schlesinger, W.H.; Jasechko, S. Transpiration in the global water cycle. *Agric. For. Meteorol.* **2014**, *189*, 115–117. [\[CrossRef\]](#)
116. Cavanaugh, M.L.; Kurc, S.A.; Scott, R.L. Evapotranspiration partitioning in semiarid shrubland ecosystems: A two-site evaluation of soil moisture control on transpiration. *Ecohydrology* **2011**, *4*, 671–681. [\[CrossRef\]](#)
117. Schlaepfer, D.R.; Ewers, B.E.; Shuman, B.N.; Williams, D.G.; Frank, J.M.; Massman, W.J.J.; Lauenroth, W.K. Terrestrial water fluxes dominated by transpiration: Comment. *Ecosphere* **2016**, *5*, 1–9. [\[CrossRef\]](#)
118. Nichols, W.D. Estimating discharge of shallow groundwater by transpiration from greasewood in the northern great basin. *Water Resour. Res.* **1993**, *29*, 2771–2778. [\[CrossRef\]](#)
119. Nichols, W.D. Groundwater discharge by phreatophyte shrubs in the great basin as related to depth to groundwater. *Water Resour. Res.* **1994**, *30*, 3265–3274. [\[CrossRef\]](#)
120. Oliveira, R.S.; Dawson, T.E.; Burgess, S. Hydraulic redistribution in three Amazonian trees. *Oecologia* **2005**, *145*, 354–363. [\[CrossRef\]](#)
121. Amenu, G.G.; Kumar, P. A model for hydraulic redistribution incorporating coupled soil-root moisture transport. *Hydrol. Earth Syst. Sci.* **2008**, *12*, 55–74. [\[CrossRef\]](#)
122. Nepstad, D.C.; Carvalho, C.D.; Davidson, E.A.; Jipp, P.H.; Lefebvre, P.A.; Negreiros, G.H.; Silva, E.D.D.; Stone, T.A.; Trumbore, S.E.; Vieira, S. The role of deep roots in the hydrological and carbon cycles of Amazonian forests and pastures. *Nature* **1994**, *372*, 666–669. [\[CrossRef\]](#)
123. Maraux, F.; Lafolie, F. Modeling Soil Water Balance of a Maize-Sorghum Sequence. *Soil Sci. Soc. Am. J.* **2011**, *62*, 75–82. [\[CrossRef\]](#)
124. Kleidon, A.; Heimann, M. Assessing the role of deep rooted vegetation in the climate system with model simulations: Mechanism, comparison to observations and implications for Amazonian deforestation. *Clim. Dyn.* **2000**, *16*, 183–199. [\[CrossRef\]](#)
125. Saleska, S.R.; Didan, K.; Huete, A.R.; da Rocha, H.R. Amazon forests green-up during 2005 drought. *Science* **2007**, *318*, 612. [\[CrossRef\]](#)
126. Liu, T.; Luo, Y. An empirical approach simulating evapotranspiration from groundwater under different soil water conditions. *Environ. Earth Sci.* **2012**, *67*, 1345–1355. [\[CrossRef\]](#)

127. Schmid, W.; Hanson, R.T.; Iii, T.M.; Leake, S. User guide for the Farm Process (FMP1) for the U.S. Geological Survey's modular three-dimensional finite-difference ground-water flow model, MODFLOW-2000. In *Book 6: Modeling Techniques, Section A. Ground-Water*; The U.S. Geological Survey Office of Ground Water, Ground-Water Resources Program: Reston, VA, USA, 2006; Chapter 17.
128. Mermoud, A.; Morelseytoux, H.J. Modélisation et observation du flux hydrique vers la surface du sol depuis une nappe peu profonde. *J. Cardiovasc. Pharmacol.* **1989**, *4*, 11–23.
129. Yuan, G.F.; Luo, Y.; Shao, M.A.; Zhang, P.; Zhu, X.C. Evapotranspiration and its main controlling mechanism over the desert riparian forests in the lower Tarim river basin. *Sci. China Earth Sci.* **2015**, *58*, 1032–1042. [\[CrossRef\]](#)
130. Yue, W.; Wang, T.; Franz, T.E. Spatiotemporal patterns of water table fluctuations and evapotranspiration induced by riparian vegetation in a semiarid area. *Water Resour. Res.* **2016**, *52*, 1948–1960. [\[CrossRef\]](#)
131. Zhang, W.J. Study on the Evapotranspiration and Water Balance of Lake Basin in the Hinterland of Badain Jaran Desert. Master's Thesis, Lanzhou University, Lanzhou, China, 2020. (In Chinese with English abstract)
132. Wondzell, S.M.; Gooseff, M.N.; McGlynn, B.L. An analysis of alternative conceptual models relating hyporheic exchange flow to diel fluctuations in discharge during baseflow recession. *Hydrol. Process.* **2010**, *24*, 686–694. [\[CrossRef\]](#)
133. Jia, W.H.; Yin, L.H.; Zhang, M.S.; Zhang, J.; Zhang, X.X.; Gu, X.F.; Dong, J.Q. Modified method for the estimation of groundwater evapotranspiration under very shallow water table conditions based on diurnal water table fluctuations. *J. Hydrol.* **2021**, *597*, 126193. [\[CrossRef\]](#)
134. Diouf, O.A.; Weihermüller, L.; Diedhiou, M.; Vereecken, H.; Cissé Faye, S.C.; Faye, S.; Sylla, S.N. Modelling groundwater evapotranspiration in a shallow aquifer in a semi-arid environment. *J. Hydrol.* **2020**, *587*, 124967. [\[CrossRef\]](#)
135. Zhao, K.Y.; Jiang, X.W.; Wang, X.S.; Wan, L. Restriction of groundwater recharge and evapotranspiration due to a fluctuating water table: A study in the Ordos Plateau, China. *Hydrogeol. J.* **2020**, *2*, 1–11. [\[CrossRef\]](#)
136. Zhu, Y.; Ren, L.; Skaggs, T.H.; Lue, H.; Yu, Z.; Wu, Y.; Fang, X. Simulation of *Populus euphratica* root uptake of groundwater in an arid woodland of the Ejina Basin, China. *Hydrol. Process.* **2010**, *23*, 2460–2469. [\[CrossRef\]](#)
137. McDonald, M.G. *A Modular Three-Dimensional Finite-Difference Groundwater Flow Model*; Techniques of Water-Resources; U. S. Geological Survey: Reston, VA, USA, 1988.
138. Banta, E.R. MODFLOW-2000, the U.S. Geological Survey Modular Ground-Water Model—Documentation of Packages for Simulating Evapotranspiration with a Segmented Function (EST1) and Drains with Return Flow (DRT1); The U.S. Geological Survey in cooperation with the Colorado Water Conservation Board and the Colorado Division of Water Resources: Reston, VA, USA, 2000.
139. Warrick, W.A. Additional solutions for steady-state evaporation from a shallow water table. *Soil Sci.* **1988**, *146*, 63–66. [\[CrossRef\]](#)
140. Pozdniakov, S.P.; Vasilevsky, P.Y.; Wang, P. Analysis of a steady-state model of groundwater discharge in a river valley without and with evapotranspiration. *Adv. Water Resour. Res.* **2022**, *168*, 104306. [\[CrossRef\]](#)
141. Baird, K.J.; Maddock, T. III. Simulating riparian evapotranspiration: A new methodology and application for groundwater models. *J. Hydrol.* **2015**, *312*, 176–190. [\[CrossRef\]](#)
142. Ajami, H.; Maddock III, T.; Meixner, T.; Hogan, J.F.; Guertin, D.P. RIPGIS-NET: A GIS tool for riparian groundwater evapotranspiration in MODFLOW. *Groundwater* **2012**, *50*, 154–158. [\[CrossRef\]](#)
143. El-Zehairy, A.A.; Lubczynski, M.W.; Gurwin, J. Interactions of artificial lakes with groundwater applying an integrated MODFLOW solution. *Hydrogeol. J.* **2017**, *26*, 109–132. [\[CrossRef\]](#)
144. Sergey, G.; Elena, F.; Victor, S.; Vsevolod, S.; Sergey, P. Evapotranspiration capture and stream depletion due to groundwater pumping under variable boreal climate conditions: Sudogda River basin, Russia. *Hydrogeol. J.* **2018**, *26*, 2753–2767.
145. Hou, X.L.; Wang, S.Q.; Jin, X.R.; Li, M.L.; Lv, M.Y.; Feng, W.Z. Using an ETWatch (RS)-UZF-MODFLOW coupled model to optimize joint use of transferred water and local water sources in a saline water area of the North China Plain. *Water* **2020**, *12*, 3361. [\[CrossRef\]](#)
146. Famiglietti, J.S.; Wood, E.F. Multiscale modeling of spatially variable water and energy balance processes. *Water Resour. Res.* **1994**, *30*, 3061–3078. [\[CrossRef\]](#)
147. Stieglitz, M.; Rind, D.; Famiglietti, J. An efficient approach to modeling the topographic control of surface hydrology for regional and global climate modeling. *J. Clim.* **1997**, *10*, 118–137. [\[CrossRef\]](#)
148. Koster, R.D.; Ducharme, A.; Stieglitz, M.; Kumar, P.; Suarez, M.J. A catchment-based approach to modeling land surface processes in a general circulation model 1. Model structure. *Journal of Geophysical Research. Biogeosciences* **2000**, *105*, 24809–24822.
149. Gutowski, W.J., Jr.; Vorosmarty, C.J.; Person, M.; Otlés, Z.; Fekete, B.; York, J. A coupled land-atmosphere simulation program (CLASP): Calibration and validation. *J. Geophys. Res. Atmos.* **2002**, *107*, 1–17. [\[CrossRef\]](#)
150. York, J.P.; Person, M.; Gutowski, W.J.; Winter, T.C. Putting aquifers into atmospheric simulation models: An example from the mill creek watershed, northeastern Kansas. *Adv. Water Resour.* **2002**, *25*, 221–238. [\[CrossRef\]](#)
151. Liang, X.; Xie, Z.H.; Huang, M.Y. A new parameterization for groundwater and surface water interactions and its impact on water budgets with the variable infiltration capacity (VIC) land surface model. *J. Geophys. Res. Atmos.* **2003**, *108*, 1–17. [\[CrossRef\]](#)
152. Miller, N.L.; Maxwell, R.M. Development of a coupled land surface and groundwater model. *J. Hydrometeorol.* **2005**, *6*, 233–247.
153. Yeh, P.J.F.; Eltahir, E.A.B. Representation of water table dynamics in a land surface scheme. Part I: Model development. *J. Clim.* **2005**, *18*, 1861–1880. [\[CrossRef\]](#)
154. Yeh, P.J.F.; Eltahir, E.A.B. Representation of water table dynamics in a land surface scheme: Observations, models, and analyses. Representation of Water Table Dynamics in a Land Surface Scheme. *Part II Subgrid Variability. J. Clim.* **2005**, *18*, 1881–1901.



155. Cohen, D.; Person, M.; Daannen, R.; Locke, S.; Dahlstrom, D.; Zabielski, V.; Winter, T.C.; Rosenbery, D.O.; Wright, H.; Ito, E.; et al. Groundwater-supported evapotranspiration within glaciated watersheds under conditions of climate change. *J. Hydrol.* **2006**, *320*, 484–500. [[CrossRef](#)]
156. Niu, G.Y.; Yang, Z.L.; Dickinson, R.E.; Gulden, L.E.; Su, H. Development of a simple groundwater model for use in climate models and evaluation with gravity recovery and climate experiment data. *J. Geophys. Res.* **2007**, *112*, D07103. [[CrossRef](#)]
157. Fan, Y.; Miguez-Macho, G.; Weaver, C.P.; Walko, R.; Robock, A. Incorporating water table dynamics in climate modeling: 1. Water table observations and equilibrium water table simulations. *J. Geophys. Res. Atmos.* **2007**, *112*, D10125. [[CrossRef](#)]
158. Jorenush, M.H.; Sepaskhah, A.R. Modelling capillary rise and soil salinity for shallow saline water table under irrigated and non-irrigated conditions. *Agric. Water Manag.* **2003**, *61*, 125–141. [[CrossRef](#)]
159. Blin, N.; Suárez, F. Evaluating the contribution of satellite-derived evapotranspiration in the calibration of numerical groundwater models in remote zones using the EEFlux tool. *Sci. Total Environ.* **2023**, *858*, 15. [[CrossRef](#)]
160. Liu, Y.; Pereira, L.S.; Fernando, R.M. Fluxes through the bottom boundary of the root zone in silty soils: Parametric approaches to estimate groundwater contribution and percolation. *Agric. Water Manag.* **2006**, *84*, 27–40. [[CrossRef](#)]
161. Askri, B.; Bouhlila, R.; Job, J.O. Development and application of a conceptual hydrologic model to predict soil salinity within modern Tunisian oases. *J. Hydrol.* **2010**, *380*, 45–61. [[CrossRef](#)]

**Disclaimer/Publisher’s Note:** The statements, opinions and data contained in all publications are solely those of the individual author(s) and contributor(s) and not of MDPI and/or the editor(s). MDPI and/or the editor(s) disclaim responsibility for any injury to people or property resulting from any ideas, methods, instructions or products referred to in the content.